MULTI-DAY THUNDERSTORM OUTBREAKS FROM LATE MAY TO EARLY JULY 2013 IN SHERIDAN COUNTY, WYOMING

Sean T. Campbell and Chauncy J. Schultz
National Weather Service, Billings, Montana

1. Introduction

The unique topography of Sheridan County, Wyoming, makes it one of the most challenging regions within the Billings County Warning/Forecast Area (CWFA) for which to forecast the development and evolution of thunderstorms. A high degree of accuracy in thunderstorm forecasting is very important in Sheridan County, though, as it is the second most populous county in the NWS Billings CWFA, is home to the second busiest airport in the NWS Billings CWFA and is a popular destination for tourists and outdoor enthusiasts. The latter is particularly true during the late spring and early summer months due to the accessibility of the Big Horn Mountains (BHM), the Big Horn National Forest, and the city of Sheridan, with its "Old West" reputation/history and the myriad outdoor events that occur there. It just so happens that the late spring and summer months are when thunderstorm activity peaks in the NWS Billings CFWA (Spector 1999), a fact that was readily apparent in 2013.

The late May to early July 2013 timeframe featured four large thunderstorm outbreaks in Sheridan County, each occurring over a three-day period. This Technical Attachment (TA) details the synoptic-scale and mesoscale patterns that resulted in each of these thunderstorm outbreaks and provides an example of a both a severe thunderstorm event and a sub-severe thunderstorm event, including some Impact-Based Decision Support Services (IDSS) implications, within two of these outbreaks. For the purpose of this TA, a strong thunderstorm event is defined as one or more thunderstorms producing hail ≥ 0.50 inches and/or wind gusts ≥ 40 mph; essentially, a thunderstorm for which NWS Billings forecasters would issue a Significant Weather Advisory (SPS). Ultimately, the goal of this TA is to increase forecaster awareness of factors contributing to large, multi-day thunderstorm outbreaks in Sheridan County and to present some ideas about what actions to take within the IDSS process once it is determined that the potential for strong to severe thunderstorms exists in Sheridan County.

2. Background

a. Geography and Basic Thunderstorm Climatology of Sheridan County

Oriented northwest to southeast and rising to elevations of 2590 m above sea level (ASL) to just over 3960 m ASL, the BHM encompass the western one-third of Sheridan County. The eastern slopes of the BHM drop sharply to elevations ranging from 1220 m ASL to 1525 m ASL, though there is a small protrusion of the mountains eastward about 25 km south of Sheridan that may aid in thunderstorm development/organization locally due to its shape. Mostly small, hilly regions become the dominant features characterizing the eastern two-thirds of Sheridan County, where elevations range from approximately 1070 m ASL in a few valleys across eastern

and central portions of the county to over 1525 m ASL across north-central portions of the county. More than 75% of the 29,000+ residents in Sheridan County live within 35 km of the BHM. This is important to note because deep, moist convection may develop over the eastern slopes of the BHM and quickly intensify as it races into central portions of Sheridan County, leaving NWS Billings forecasters little time to warn customers and partners.

A review of lightning flash climatology from the 1990s reveals that the density of lightning flashes per square kilometer dramatically increased just east of the BHM (Fig. 1b). It is likely that this spatial distribution of lightning flashes in Sheridan County is similar on a longer time-scale for reasons that will be discussed and illustrated throughout this TA.

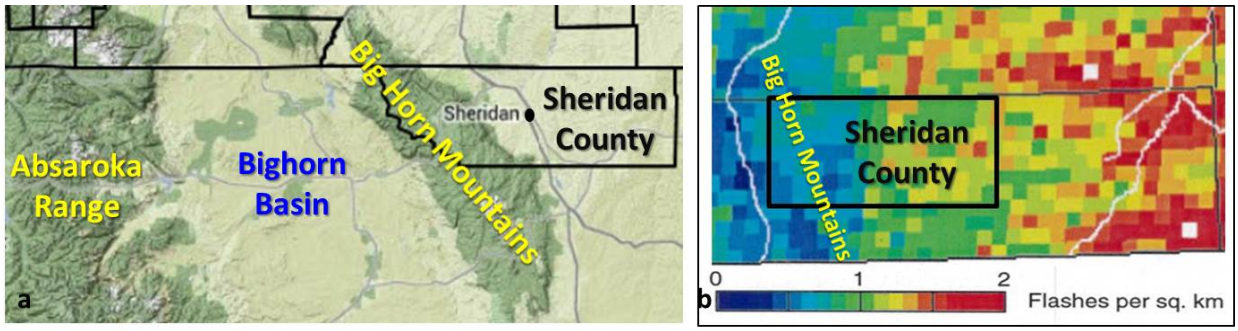

Figure 1: (a) Topographical map of northwestern Wyoming/extreme south-central Montana with Sheridan County outlined and various topographical features listed; (b) a map of lightning climatology (flashes per square km per year) from the 1990s with Sheridan County roughly outlined by the black rectangular box. Note that lightning flashes increase rapidly just east of the BHM. Figure 1b source: Ronald Holle, National Severe Storms Laboratory (NSSL).

b. Effects of the BHM on Thunderstorm Development and Evolution

i. Thermally-Direct Circulation

By late May/early June, a majority of the snow has already melted in the higher elevations of the BHM in Sheridan County, exposing the rocky peaks. During the daytime, the rocky slopes quickly warm, becoming an elevated heat source (Banta 1990, Orville 1965, 1968). Air next to the mountain slopes becomes warmer than air at the same level some distance away from the mountains (Rife 1996). This generates lower pressure over the mountains and induces a thermally direct circulation, wherein air at the surface is pulled towards the BHM and begins to flow up both the western and eastern slopes. If the circulation is strong enough, convergence occurs over the mountains (Fig. 2a). The addition of synoptic-scale and/or mesoscale forcing, such as upper-level divergence or positive vorticity advection ahead of a mid-level shortwave trough will act to increase flow up the BHM, thereby enhancing both convergence and the potential for updraft formation/vertical cloud growth over the BHM.

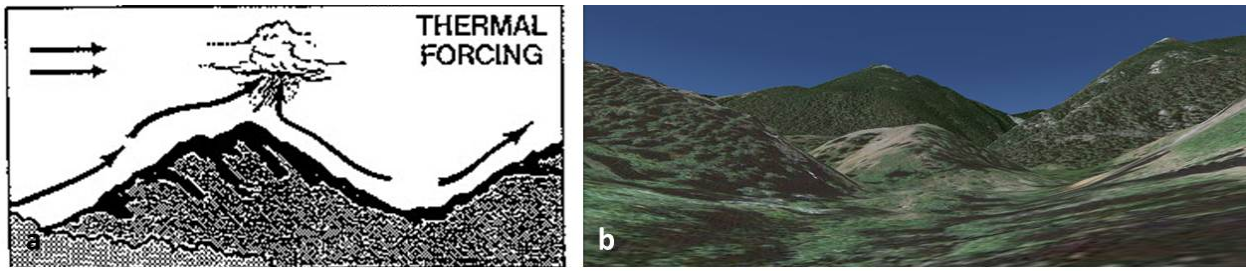

Figure 2: (a) Example of mountain-induced thermal forcing and (b) a GoogleEarth view of a portion of the steep eastern slopes of the BHM in Sheridan County, facing southwest. Figure 2a adapted from Banta (1990).

ii. Airmass Differences

Airmasses on both sides of the BHM can be quite different. To the west of the BHM sits the Big Horn Basin (BHB), with elevations generally ranging from 1220 m ASL to 1525 m ASL. The BHB, which is approximately 160 km wide, sits between the Absaroka Range to the west and the BHM to the east (Fig. 1a). Because atmospheric disturbances tend to move generally from west to east across the region, much of the precipitation associated with these systems is "rained out" in the Absaroka Range west of the BHB, effectively leaving the BHB in a precipitation shadow. West to southwest downslope flow enhances the precipitation shadow effect at times, decreasing moisture content in the air within the BHB. With no significant synoptic-scale or mesoscale forcing present, the relatively dry air in the BHB may be ingested into the thermally-direct circulation over the BHM, inhibiting moist convection.

East of the BHM, the airmass may be quite moist in the low- to mid-levels as Gulf of Mexico moisture and moisture resulting from evapotranspiration of crops across the Plains states may be advected from the east and southeast. Latent heat release may be increased and buoyancy may be enhanced as this moist air is pulled up the eastern slopes of the BHM by the thermally-direct circulation.

Given additional forcing, instability and shear, the mixing of the two airmasses over the top of the BHM may produce convection, with the dry air from the west entraining into developing thunderstorms. It is likely that this increases the potential for strong downdrafts and/or the development of a somewhat steady-state cold pool that can help accelerate the thunderstorms as they move towards the more populated region of central Sheridan County.

iii. Potential Vorticity Influences

Upper-level potential vorticity advection may strengthen lee cyclogenesis (Mattocks and Bleck 1986), deepen a lee trough or enhance development of a wave along a stationary surface boundary east of a mountain range. Any of these three scenarios would increase upward vertical motion just east of the BHM. Also, increasing west or southwesterly winds aloft, which can occur ahead of an approaching shortwave or upper-level jet streak, may also push the thermally-direct circulation off of the mountains and help to tilt any updraft that develops

(Orville 1968). The thermally-direct circulation over the BHM, then, may be shifted or elongated towards the lee side of the mountains if an approaching shortwave/atmospheric disturbance is strong enough. This may increase the potential for rapid thunderstorm development over the eastern slopes of the BHM.

Additionally, the concept of conservation of potential vorticity applies. Air ahead of an approaching atmospheric disturbance moving up the western side of the BHM is compressed, then, is rapidly stretched/expanded when moving down the steep eastern slopes (Fig. 2b). Because the ratio of absolute vorticity to the depth of the air column remains constant, the absolute vorticity of the air is reduced when it moves up the western slopes as decreasing relative vorticity leads to reduced cyclonic spin, weakening upward vertical motion. As the air descends down the eastern slopes, the absolute vorticity of the air increases because the increasing relative vorticity leads to faster cyclonic spin (Holton 1992). This enhances upward vertical motion directly over and just east of the steep eastern side of the BHM.

iv. Upward Propagating Flow Effects

Thunderstorms generated over the BHM may also be enhanced on the lee side by the combined effects of upward motion associated with an upward-propagating wave caused by flow over the mountains and the low-level upslope flow (Houze 1993). Under favorable environmental conditions, thunderstorms that develop in such a manner may organize into mesoscale convective systems (MCSs) and continue to propagate eastward (Houze 1993). Indeed, MCSs were observed from Sheridan County eastward during all four multi-day thunderstorm outbreaks in 2013 and were observed by NWS Billings forecasters in thunderstorm outbreaks during previous years.

3. General Overview of the Multi-Day Thunderstorm Outbreaks

Prior to the late May to early July 2013 convective activity, above average precipitation occurred from April to mid-May across much of south-central Montana and northern Wyoming. Sheridan County was no exception, as some locations received greater than three inches more than average for that time period. Near-saturation of the soil resulted from the above average precipitation, enabling vegetation through the county to grow and ensuring that low-level moisture was present across the area. This low-level moisture, especially east of the BHM, where surface dewpoints remained from near 10°C to over 16°C (at times) from late May through early July, played a large role in thunderstorm development during that timeframe.

Dates of the four thunderstorm outbreaks were 26 to 28 May, 11 to 13 June, 20 to 22 June and 6 to 8 July. With the exception of 22 June, when convection developed during the late morning/early afternoon, convection during the 12 thunderstorm (event) days impacted Sheridan County during the late afternoon/evening hours at various times between 2100 UTC (3:00 pm) and 0500 UTC (11:00 pm). This indicates that instability was an important factor in thunderstorm development. Indeed, surface lifted indices (LIs) at or less than -2°C were observed during or just prior to 9 of the 12 events and surface-based (SB) CAPE values greater

than 500 J kg^{-1} east of the BHM were present in 11 of the 12 events. Strong mid- and upper-level forcing were also very important, as both a mid-level shortwave (either at 500 mb or at 700 mb) and upper-level divergence were evident during all 12 events, with an upper-level divergence "bullseye" discernible at 300 mb in 8 of the 12 events. Effective bulk shear (EBS) of 30 kts or greater, sufficient for at least a marginal supercell (Thompson et al. 2007), was also evident during all 12 events.

The 26 to 28 May and 11 to 13 June outbreaks occurred ahead of deep upper-level troughs, with strong upper level forcing. A substantial amount of hail (Fig. 3a, c), strong wind (Fig. 3b) and heavy rain (Fig. 3d) reports were received during these two events. Significant damage occurred due to the hail and winds; flash flooding was reported in the city of Sheridan.

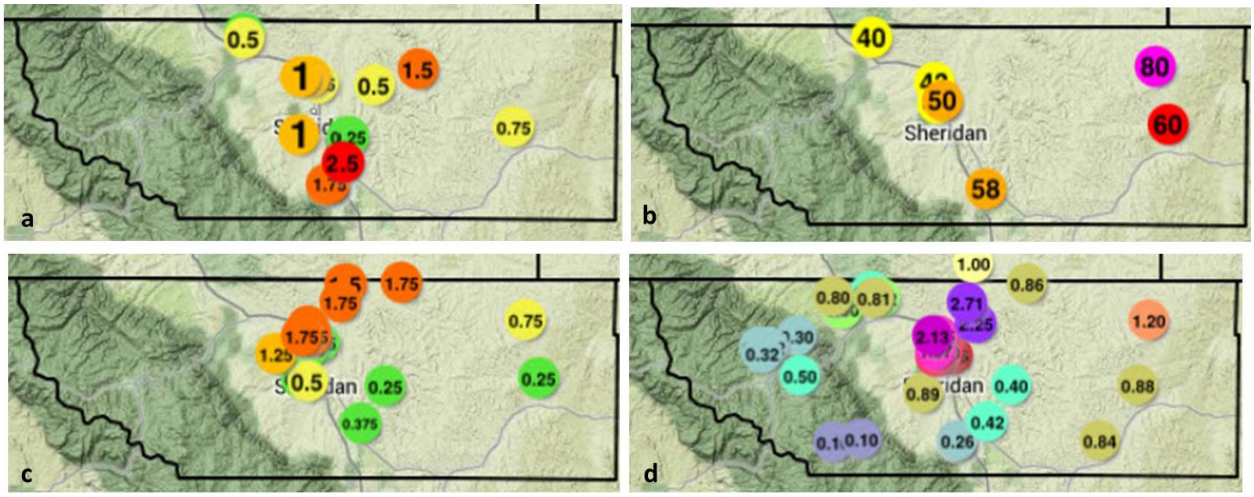

Figure 3: (a) Hail reports in inches in diameter from 26 to 28 May 2013, (b) convective wind reports in mph from 11 to 13 June 2013, (c) hail reports in inches in diameter from 11 to 13 June 2013 and (d) rainfall reports in inches from 11 to 13 June 2013. Source: NWS Billings.

Thunderstorms from 20 to 22 June also developed ahead of an upper-level trough, but there was only a relatively small pocket of cold air in the base of this trough, indicative of a cold core low in the process of cutting off and weakening as it moved towards the region. Only one sub-severe hail report was received (Fig. 4a) and a majority of the reports during this multi-day event were of rainfall of less than one inch (Fig. 4b). An example of deep moist convection caused by shortwave activity in southwesterly flow, the 6 to 8 July thunderstorm outbreak produced a few sub-severe hail reports (Fig. 4c) and a few sub-severe and severe convective wind reports (Fig. 4d).

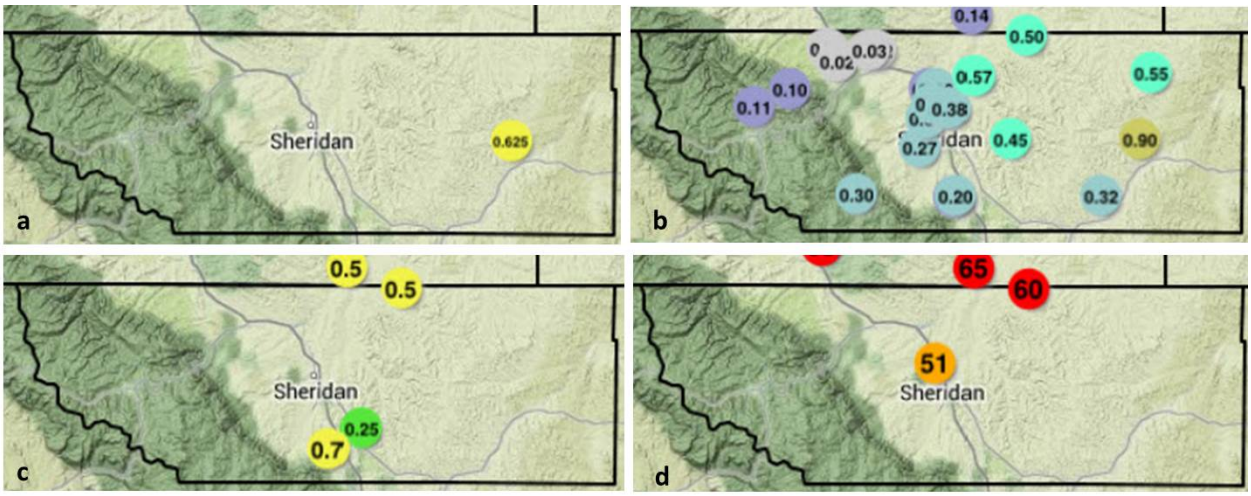

Figure 4: (a) Hail report in inches in diameter from 20 to 22 June 2013, (b) rainfall reports in inches from 20 to 22 June 2013, (c) hail reports in inches in diameter from 6 to 8 July 2013 and (d) convective wind reports in mph from 6 to 8 July 2013. Source: NWS Billings.

An after-the-fact review of SPC Storm-Scale Ensemble of Opportunity (SSEO) products, as described by Jirak et. al. (2012), showed that prior to all 12 convective events, at least one member of the SSEO forecast convection capable of generating reflectivity values greater than 40 dBZ. SSEO products also forecast at least a slight chance of updraft speeds greater than or equal to 10 m s^{-1} (22 mph) and updraft helicity values greater than or equal to 25 m^2 s^{-2} in or within 40 km of Sheridan County during 10 of the 12 events.

4. Significant Thunderstorm Event Examples

a. 13 June 2013 Thunderstorm Event

i. Overview

A supercell produced severe hail up to 1.75 inches in diameter (golf ball size) along a path with a length of approximately 65 km across central and northern Sheridan County during the mid-afternoon of 13 June, as well as one spotter-estimated 58 mph wind gust in the northeast portion of the county (National Climatic Data Center [NCDC] *Storm Data* 2013). Large hail affected the northwest side of the city of Sheridan. Convection incipient to the supercell originated over the mountains of northwestern Wyoming around 1700 UTC, and the supercell developed in the BHB to the southwest of Greybull, Wyoming, around 1925 UTC. Hail ranging in size from 0.75 to 1.00 inches in diameter (penny to quarter size) was reported in the BHB between 1950 and 2020 UTC (NCDC *Storm Data* 2013), when the supercell displayed an operator- and algorithm-defined mesocyclone, mid-level echo overhang, and a strong reflectivity gradient on the inflow side of the storm. The storm maintained at least weak supercell signatures as it crossed the west side of the BHM, but maximum reflectivity and mesocyclone strength both diminished as the storm ascended the western side of the mountain range, only to increase once more as the storm began descending into the foothills on the

eastern side of the BHM. The supercell rapidly intensified just southwest of Sheridan, Wyoming, and displayed a notable mesocyclone and an intense reflectivity core with maximum reflectivity values around 70 dBZ (and 50 dBZ values above 9145 m above ground level) as it produced severe weather across the lower elevations of Sheridan County east of the BHM between approximately 2100 and 2300 UTC. The lifecycle of the supercell was approximately 3.5 hours, just short of the 4-hour temporal minimum necessary for classification as a long-lived supercell (Bunkers et al. 2006). The evolution of the 13 June supercell is shown in Fig. 5.

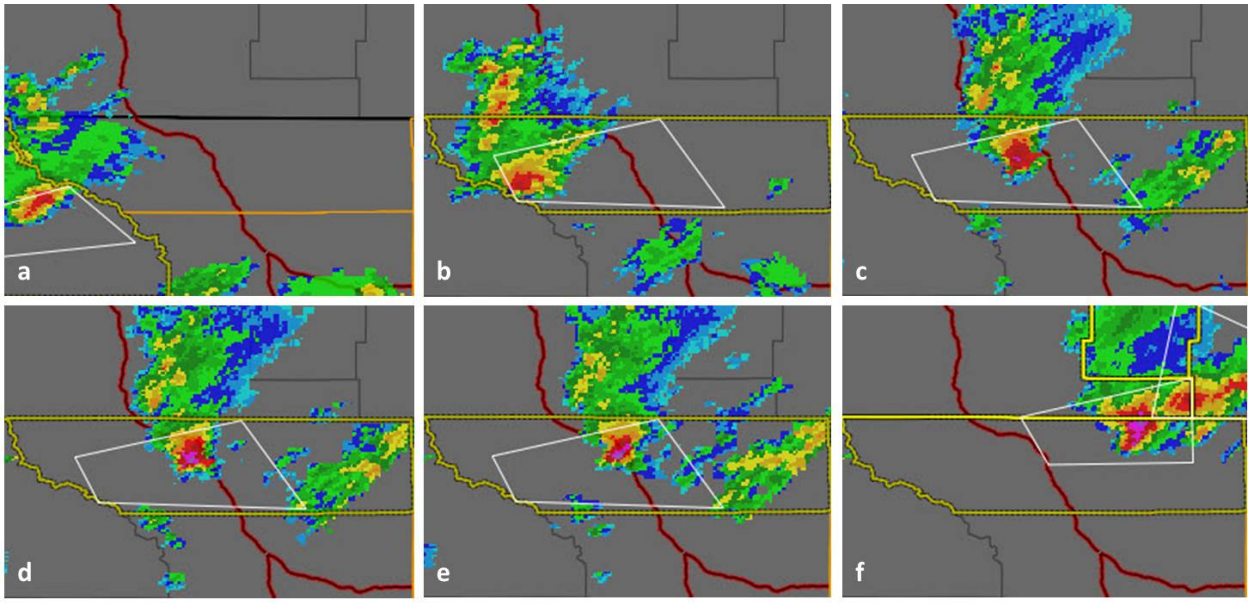

Figure 5: WSR-88D KBLX Composite Reflectivity with severe thunderstorm polygons, centered on Sheridan County, Wyoming, from (a) 2030 UTC, (b) 2050 UTC, (c) 2120 UTC, (d) 2125 UTC, (e) 2130 UTC and (f) 2200 UTC on 13 June 2013. Source: Iowa Environmental Mesonet (IEM)'s NEXRAD Composite Reflectivity Archives.

ii. Pre-Existing Environmental Conditions

The convection which formed over northwestern Wyoming in the late morning on 13 June developed in diffluent/divergent southwest flow aloft downstream of an upper-level trough, which had its axis over central Washington and Oregon by mid-afternoon. The 2100 UTC objectively-analyzed 700 mb analysis (Fig. 6b) suggests that a mid-level shortwave trough embedded in the southwest flow aloft may have aided the convective development and sustenance across the region, as well. In the BHB, surface temperatures were around 27°C and dewpoints were just under 10°C at 1900 UTC, contributing to SBCAPE of 500 J kg^{-1} based on RAP-based objective analysis data. EBS was near 30 kts (not shown). The Remote Automated Weather Station (RAWS) at Burgess Junction, Wyoming, at an elevation of 2360 m ASL and in the immediate inflow region of the supercell, reported a surface temperature and dewpoint of 20°C and 4°C, respectively, at 2000 UTC. This likely decreased the buoyancy for surface-based parcels as the supercell ascended the BHM, consistent with the reduction in intensity observed on radar and lack of severe weather reports even as the storm affected one of the few places

with a permanent population in the BHM at Burgess Junction. In addition, the height of the storm likely decreased as it ascended the BHM, owing to a reduction in SBCAPE and equilibrium level as inflow ingested cooler and drier surface conditions. Even if the equilibrium level remained constant, the storm would likely have become shorter as its base increased with the elevation of the terrain. EBS values would have increased with a shorter storm (Thompson et al. 2007). Weisman and Klemp (1982, 1984) discussed the presence of an optimum CAPE-shear balance for supercells, and McCaul and Weisman (2001) noted that excessive bulk shear tends to destroy storms. Thus, the increasing EBS encountered by the supercell as it ascended the BHM may have been detrimental to its strength and may account for the observed weakening of the storm. The decrease in relative vorticity encountered upon the supercell's ascension of the BHM is another possible reason for its weakening.

In the lower elevations of Sheridan County, east of the BHM, surface moisture was locally maximized during the afternoon with dewpoints of 16°C to 17°C in central and eastern parts of the county. A surface Θ_e ridge with values greater than 345K was also present (Fig. 6c). In addition, EBS was around 50 kts (Fig. 6d), which is near the 75th percentile of EBS associated with nontornadic supercells (Thompson et al. 2006). Given the favorable EBS and increasing buoyancy (SBCAPE of 2000 to 2500 J kg^{-1}; Fig. 6e), as well as the increase in relative vorticity over the steep eastern slopes of the BHM, it is not surprising that the supercell rapidly strengthened as it descended the BHM and maintained its strength as it crossed Sheridan County. The storm encountered an axis of relatively higher DCAPE values in the northeast portion of Sheridan County (Fig. 6f), corresponding to the lone severe wind gust reported during this event. High DCAPE values are useful in estimating maximum convective wind gust strength (Doswell 1993, Gilmore and Wicker 1998, and Evans and Doswell 2000). The supercell weakened rapidly after exiting the county around 2300 UTC as it moved into an airmass containing increasing surface-based convective inhibition near -75 J kg^{-1} (not shown).

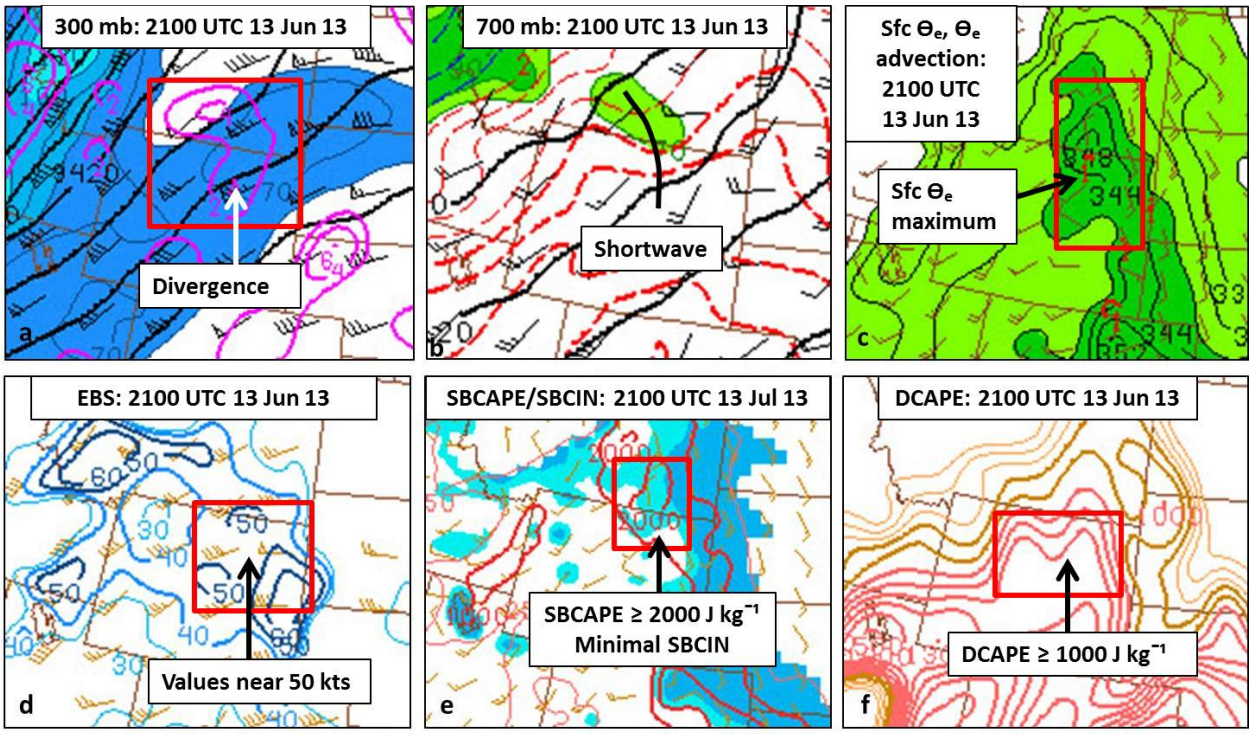

Figure 6: (a) 300 mb height/divergence/wind, (b) 700 mb height/wind/temperature in °C/700 - 500 mb mean relative humidity (fill), (c) surface Θ_e (fill)/advection (°C per hr), (d) EBS, (e) SBCAPE (contour) and SB convective inhibition (CIN) (J kg^{-1}, shaded at 25 and 100), and (f) DCAPE, all at 2100 UTC on 13 June 2013. Source: SPC's Mesoscale Analysis Archive.

SSEO convective forecasts prior to the 13 June event indicated that there was a moderate chance of thunderstorm activity in and near Sheridan County during the timeframe that thunderstorms impacted Sheridan County (Fig. 7a). The probability of stronger thunderstorms, as indicated by the SSEO's forecast of updraft speeds greater than 10 m s^{-1}, was highest from Sheridan north and east (Fig. 7b). Remarkably, this is where the strongest thunderstorms, with hail 1.00 inch or greater, tracked (Fig. 5d-f).

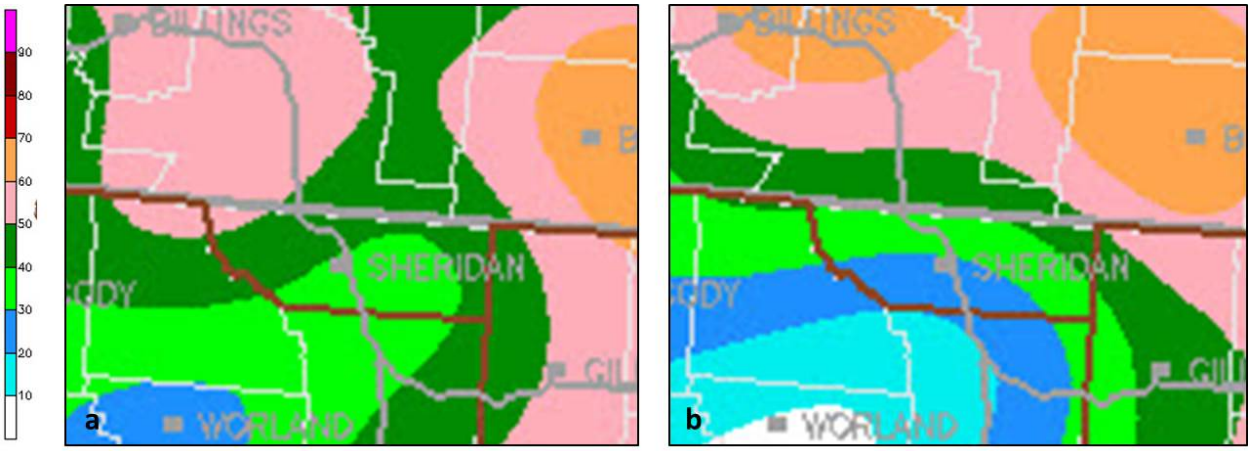

Figure 7: (a) 0000 UTC 13 June 2013 SSEO forecasts of 3-hour probability of reflectivity values > 40 dBZ and (b) 3-hr probability of updrafts > 10 m s^{-1} for Sheridan County and the surrounding area, valid from 2100 UTC 13 June 2013 to 0000 UTC 14 June 2013. Source: SPC's SSEO.

b. 6 - 7 July 2013 Thunderstorm Event

i. Overview

A disorganized area of showers and embedded weak thunderstorms (Fig. 8a) rapidly organized into a line, intensified and raced eastward as the convection descended the eastern slopes of the BHM and moved into the adjacent plains on 7 July (Fig. 8b-f). As the thunderstorms intensified east of the BHM, maximum reflectivity values over 50 dBZ quickly topped 6100 m AGL in the cells that produced wind gusts of 51 mph at the Sheridan County airport and hail up to 0.70 inches in diameter (dime sized) near Story, Wyoming. Later, minor flooding was reported in eastern Sheridan County as several of the cells within the line merged into a supercell that generated rainfall rates greater than 4.00 inches per hour for several minutes as it propagated eastward. Evidence of such evolution on a stronger scale occurred during the 13 June event (Fig. 5).

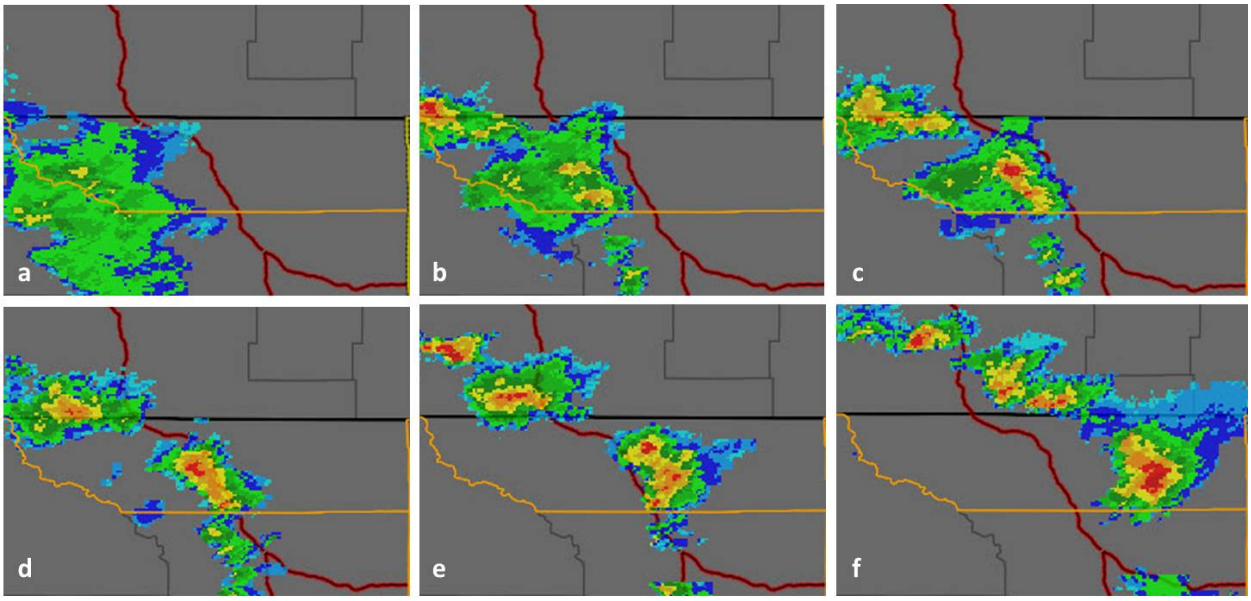

Figure 8: NEXRAD KBLX Composite Reflectivity, centered on Sheridan County, Wyoming, from (a) 0020 UTC, (b) 0050 UTC, (c) 0100 UTC, (d) 0110 UTC, (e) 0130 UTC and (f) 0200 UTC on 7 July 2013. Source: IEM's NEXRAD Composite Reflectivity Archives.

ii. Pre-Existing Environmental Conditions

Between 1800 UTC and 2300 UTC on 6 July, several clusters of showers and sub-severe thunderstorms developed over the Absaroka Range of northwestern Wyoming in divergent upper-level southwest flow ahead of mid-level shortwave activity. These thunderstorm clusters then moved east into the BHB, where surface temperatures ranged from 27°C to 32°C and surface dewpoints ranged from near 4°C to near 13°C. Where dewpoints were lowest, across the southern two-thirds of the BHB, the airmass was more stable, thus thunderstorm clusters remained weak and disorganized. Where dewpoints were highest, across the northern third of the BHB, the airmass was more unstable, thus at least two thunderstorms within one of the clusters intensified enough between 2300 UTC on 6 July and 0000 UTC on 7 July to warrant the issuance of a severe thunderstorm warning. As the thunderstorms began to ascend the BHM from the west, they weakened, likely for the same reasons the severe thunderstorm on 13 June weakened as it ascended the western slopes of the BHM. By 0030 UTC, the convective clusters had formed into an elongated line over the BHM with weak reflectivity values observed on radar. Surface temperatures in the BHM just prior to the elongated line cresting the mountains ranged from 13°C to 18°C, though dewpoints generally ranged from 10°C to 13°C, thus buoyancy was somewhat reduced over the BHM as compared to when thunderstorms were moving across the northern portion of the BHB. Between 0100 UTC and 0110 UTC on 7 July, the thunderstorms began to move over the steep eastern slopes of the BHM (where absolute vorticity rapidly increases due to stretching) into the adjacent foothills and quickly intensified (Fig. 8b-c). The line of thunderstorms maintained its enhanced strength beyond 0200 UTC as it moved into eastern Sheridan County.

The primary forcing mechanisms for this event appear to be upper level divergence in the right entrance region of a jet maximum (Fig. 9a) and mid-level shortwave activity (Fig. 9b) in southwesterly flow aloft. Shortly before convective initiation, EBS values of at least 30 kts were evident (Fig. 9d) and SBCAPE values of approximately 1000 J kg^{-1} were in place just east of the BHM (Fig. 9e). As thunderstorms were in the process of forming, pooling of surface dewpoints close to 16°C was observed just east of the BHM and a Θ_e ridge with values reaching 347K was in place just east of the BHM (Fig. 9c). The potential for strong convective winds was also high, with DCAPE values of 1000 J kg^{-1} or greater present (Fig. 9f).

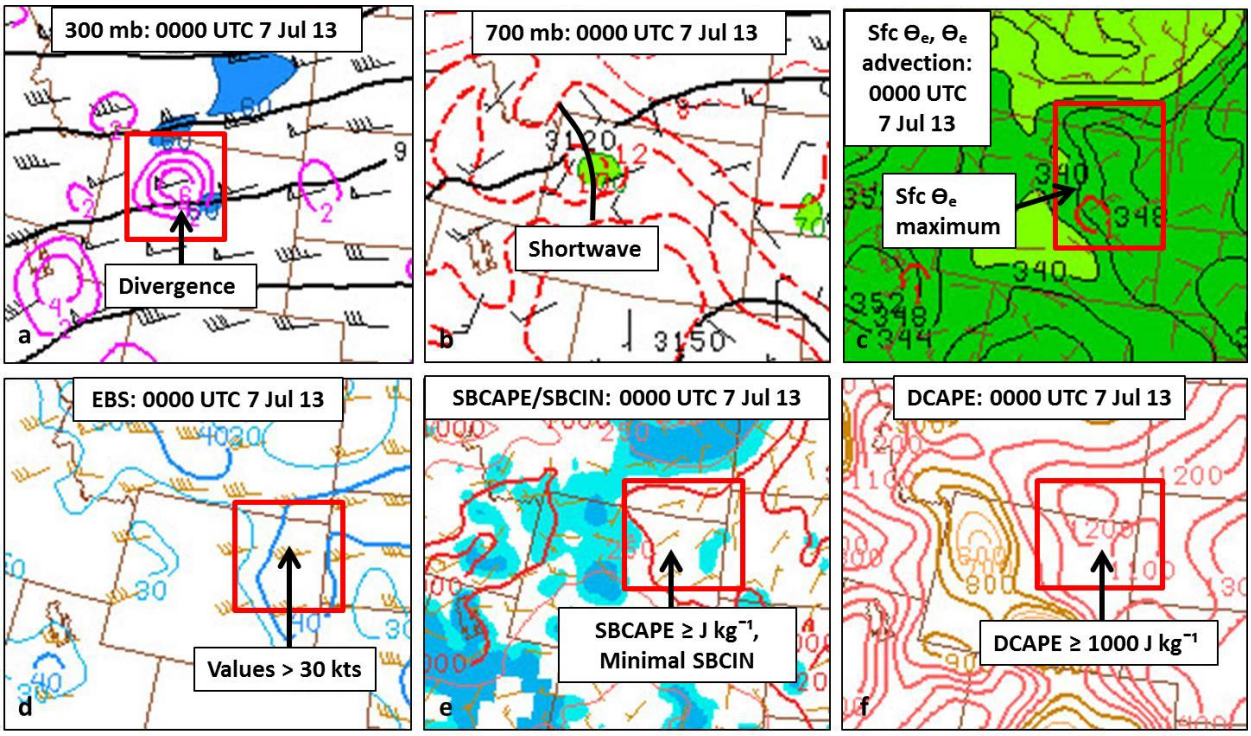

Figure 9: (a) 300 mb height/divergence/wind, (b) 700 mb height/wind/temperature in °C/700 - 500 mb mean relative humidity (fill), (c) surface Θ_e (fill)/advection (°C per hr), (d) EBS, (e) SBCAPE (contour) and SBCIN (J kg^{-1}, shaded at 25 and 100), and (f) DCAPE, all at 0000 UTC on 7 July 2013. Source: SPC's Mesoscale Analysis Archive.

SSEO convective forecasts prior to the 6 July event indicated that there was at least a slight chance of thunderstorm activity in and near Sheridan County during the timeframe that thunderstorms impacted Sheridan County (Fig. 10a). There was also a slight chance of strong thunderstorms, essentially from Sheridan west, as indicated by the SSEO's forecast of updraft speeds greater than 10 m s^{-1} (Fig. 10b). Interestingly, thunderstorms rapidly intensified within this area (Fig. 8b-c).

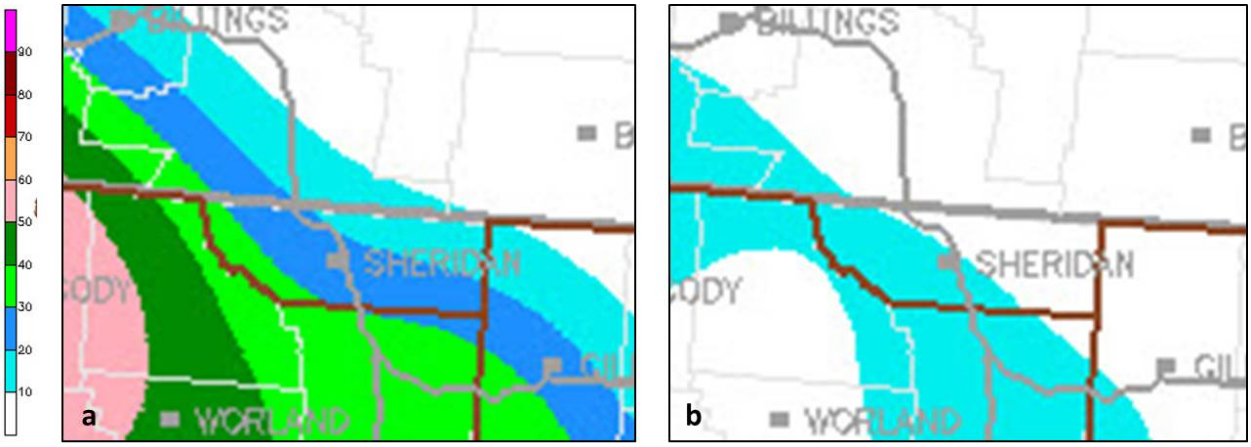

Figure 10: (a) 0000 UTC 6 July 2013 SSEO forecasts of 3-hour probability of reflectivity values > 40 dBZ and (b) 3-hr probability of updrafts > 10 m s^{-1} for Sheridan County and the surrounding area, valid from 0000 UTC 7 July 2013 to 0300 UTC 7 July 2013. Source: SPC's SSEO.

c. IDSS Challenges: 13 June 2013 and 6 - 7 July 2013

Warning forecasters for Sheridan County were faced with two big challenges on 13 June and from 6 - 7 July. The first was determining how convection would evolve as it crossed the BHM and descended into the lower elevations of Sheridan County, where conditions were favorable for rapid thunderstorm development/re-intensification. A second challenge was determining which IDSS/social media products to issue and when to issue them.

Leading up to the events, pattern recognition and probabilistic output from convective allowing forecast models was used to help forecasters assess the threat of strong to severe thunderstorms across Sheridan County. Based on pattern recognition, forecasters were able to utilize text-based hazardous weather outlooks to discuss a generic threat of severe thunderstorms that included northern Wyoming seven days in advance of the 13 June event and five to six days in advance of the 6 - 7 July convective episode, respectively. Generalized graphical forecast products and social media posts were also provided to decision-makers and the public in advance of the events, alerting them to the potential of strong to severe thunderstorms in Sheridan County.

On the day of each outbreak, SSEO output provided forecasters with increasing confidence that Sheridan County could be impacted by strong to severe thunderstorms, so forecasters were prepared to provide enhanced services even before convection began. In each of these cases, convection initially erupted well west of the Billings CWFA, giving forecasters significant time to monitor its evolution. As convection moved up the western slopes of the BHM, it weakened to sub-severe limits. The 13 June thunderstorm maintained its supercell structure to some extent, while thunderstorms during the 6 - 7 July event became an elongated area of weaker convection.

After the convection crested the BHM and began to move over the eastern slopes, it rapidly intensified. Forecasters were quick to note the intensification on radar (though the atmosphere below 2135 m AGL is not well-sampled by Doppler weather radar in the Sheridan region), thus applicable IDSS products - a severe thunderstorm warning on 13 June and an SPS on 7 July - were issued even before convection moved from the eastern slopes of the BHM into the more populated areas of Sheridan County. These prompt actions provided over 20 minutes of lead time prior to the first reports of 1.00 inch hail (13 June) and wind gusts over 50 mph (7 July) in the Sheridan area. The expectation and subsequent occurrence of storm intensification over and just east of the BHM also allowed for timely and accurate updates to aviation forecasts for the Sheridan County airport and enabled pointed, specific social media posts to be made before impacts occurred.

5. Conclusions and IDSS Implications

To summarize, all four thunderstorm outbreaks described in this TA occurred within southwesterly flow aloft ahead of slow-moving or stationary upper-level troughs and did so over three-day periods, indicating that the potential for thunderstorms can exist for several days in a row. Complex orographic processes/interactions such as an eastward elongation of BHM-induced thermally-forced convergence and an increase in absolute vorticity over the steep eastern slopes of the BHM appeared to contribute to the convective development. Other factors leading to rapid thunderstorm development over and just east of the BHM included upper-level divergence, mid-level shortwave forcing, instability (increasing mid-level cold air advection and surface LIs of at least -2°C) and increasing moisture east of the BHM (surface Θ_e ridging, surface dewpoints ranging from near 10°C to near 18°C and increasing PWATs). In terms of convective parameters, SBCAPE values of at least 500 J kg^{-1} and EBS values of at least 30 kts just east of the BHM further enhanced the potential for organized convection. Future thunderstorm outbreaks and additional research may reveal other important factors that can alert forecasters to a heightened threat of strong to severe convection in Sheridan County.

If environmental factors/processes such as those identified in this TA are evident at the beginning of a forecast shift or appear to be more likely as a shift progresses, forecaster confidence in thunderstorm development over and just east of the BHM may be increased. Confidence in thunderstorm potential within Sheridan County may be further bolstered if, during an analysis at the beginning of the forecast shift (and reanalysis throughout the shift), probabilistic output derived from individual, deterministic convection-allowing models forecast models, such as those comprising SPC's SSEO, the Short Range Ensemble Forecast system and/or deterministic, convection-allowing models such as the High-Resolution Rapid Refresh.

When analysis confirms that the potential for strong to severe thunderstorms is enhanced in Sheridan County, a forecaster should notify neighboring NWS forecast offices such as Riverton, Wyoming, and Rapid City, South Dakota, as well as the Storm Prediction Center. At this point, creating or updating IDSS/social media products should occur so NWS Billings partners/customers are made aware of an enhanced thunderstorm threat. If environmental conditions point to an imminent thunderstorm outbreak in Sheridan County, forecasters should

keep a very close watch on upper-level divergence "bullseyes", mid-level shortwaves, and other synoptic-scale and mesoscale forcing mechanisms as they move across northwestern Wyoming and interact with the BHM. Because thunderstorms can develop so rapidly over and just east of the BHM, then race quickly into a populated region, many IDSS and social media products/actions may need to be coordinated and/or issued in a very short period of time. Thus, it may be beneficial for the Lead Forecaster to assign two or more forecasters to Sheridan County IDSS and collaboration duties until the thunderstorm threat there has passed.

Acknowledgements

The authors thank Mike Staudenmaier, Deputy Chief, NWS Western Region Science and Technology Infusion Division, Keith Meier, NWS Billings Meteorologist-In-Charge, and Marc Singer, NWS Billings Science and Operations Officer, for reviewing this TA and for providing helpful feedback.

References

Banta, R., 1990: The role of mountain flows in making clouds. Amer. Met. Soc., Meteo. Mono. No. 45, Vol. 23, pp. 229-283: Atmospheric processes over complex terrain.

Bunkers, M. J., M. R. Hjelmfelt, and P. L. Smith, 2006: An observational examination of long-lived supercells. Part I: characteristics, evolution, and demise. *Wea. Forecasting*, **21**, 673-688.

Doswell, C. A. III, 1993: Extreme Convective Windstorms: Current understanding and research. Report of the Proceedings (1994) of the U.S.-Spain Workshop on Natural Hazards (Barcelona, Spain, 8-11 June 1993), J. Corominas and K.P. Georgakakos, Eds., pp. 44-55.

Evans, J. S., and C. A. Doswell III, 2001: Examination of derecho environments using proximity soundings. *Wea. Forecasting*, **16**, 329-342.

Gilmore, M.S., and L.J. Wicker, 1998: The influence of midtropospheric dryness on supercell morphology and evolution. *Mon. Wea. Rev.*, **126**, 943-958.

Holton, J.R., 1992: *An Introduction to Dynamic Meteorology – 3rd ed*. Academic Press, Inc., San Diego, 511 pp.

Houze, Jr., R., 1993: *Cloud Dynamics*. Academic Press, Inc., San Diego, 573 pp.

Iowa Environmental Mesonet, 2013: IEM NEXRAD Composite Base Reflectivity Archive. [Available online at http://mesonet.agron.iastate.edu/GIS/apps/rview/warnings.phtml]

Jirak, I. L., S. J. Weiss, and C. J. Melick, 2012: The SPC storm-scale ensemble of opportunity: Overview and Results from the 2012 Hazardous weather testbed spring forecasting experiment. *Preprints*, 26th Conf. Severe Local Storms, Nashville TN. Amer. Meteo. Soc., P9.137.

Mattocks, C and R. Bleck, 1986: Jet streak dynamics and geostrophic adjustment processes during the initial stages of lee cyclogenesis. *Mon. Wea. Rev.,* **114**, 2033-2056.

McCaul, E. W., and M. L. Weisman, 2001: The sensitivity of simulated supercell structure and intensity to variations in the shapes of environmental buoyancy and shear profiles. *Mon. Wea. Rev.*, **129,** 664-687.

National Climatic Data Center, 2013: *Storm Data*, **55** (6). [Available online at http://www.ncdc.noaa.gov/IPS/sd/sd.html]

Orville, H. D., 1965: A numerical study of the initiation of cumulus clouds over mountainous terrain. *J. Atmos. Sci.*, **22**, 684-699.

Orville, H. D., 1968: Ambient wind effects on the initiation and development of cumulus clouds over mountains. *J. Atmos. Sci.*, **25**, 385-403.

Rife, D., 1996: The effects of mountains and complex terrain on airflow and development of clouds and precipitation. WR-Technical Attachment 96-16.

Spector, D., 1999: Severe thunderstorm climatology in south-central and southeastern Montana. WR-Technical Attachment 99-07.

Thompson, R. L., C. M. Mead, and R. Edwards, 2007: Effective storm-relative helicity and bulk shear in supercell thunderstorm environments. *Wea. Forecasting*, **22**, 102-115.

Weisman, M., and J. Klemp, 1982: The dependence of numerically simulated convective storms on vertical wind shear and buoyancy. *Mon. Wea. Rev.*, **110,** 504-520.

Weisman, M., and J. Klemp, 1984: The structure and classification of numerically simulated convective storms in directionally varying wind shears. *Mon. Wea. Rev.*, **112,** 2479-2498.